Atmos. Chem. Phys. Discuss., 15, 27501–27538, 2015
www.atmos-chem-phys-discuss.net/15/27501/2015/
doi:10.5194/acpd-15-27501-2015

Atmospheric Chemistry and Physics Discussions

First comprehensive modelling study on observed new particle formation at the SORPES station in Nanjing, China

X. Huang[1,2], L. X. Zhou[3,4], A. J. Ding[1,2], X. M. Qi[1,2], W. Nie[1,2], M. H. Wang[1,2], X. G. Chi[1,2], T. Petaja[3], V.-M. Kerminen[3], P. Roldin[3], A. Rusanen[3], M. Kulmala[3], and M. Boy[3]

[1]Institute for Climate and Global Change Research and School of Atmospheric Sciences, Nanjing University, Nanjing, 210023, China
[2]Collaborative Innovation Center of Climate Change, Nanjing, Jiangsu Province, China
[3]Department of Physics, University of Helsinki, P.O. Box 64, 00014 University of Helsinki, Finland
[4]Helsinki University Centre for Environment, P.O. Box 65, 00014 University of Helsinki, Finland

Received: 22 July 2015 – Accepted: 12 September 2015 – Published: 13 October 2015

Correspondence to: A. J. Ding (dingaj@nju.edu.cn)

Published by Copernicus Publications on behalf of the European Geosciences Union.

Abstract

New particle formation (NPF) has been investigated intensively during the last two decades because of its influence on aerosol population and the possible contribution to cloud condensation nuclei. However, intensive measurements and modelling activities on this topic in urban metropolitans in China with frequently high pollution episodes are still very limited. This study provides results from a comprehensive modelling study on the occurrence of new particle formation events in the western part of the Yangtze River Delta region (YRD), China. The comprehensive modelling system, which combines regional chemical transport model WRF-Chem (the Weather Research and Forecasting model coupled with Chemistry) and the sectional box model MALTE-BOX (the model to predict new aerosol formation in the lower troposphere), was shown to be capable of simulating atmospheric nucleation and subsequent growth. Here we present a detailed discussion of three typical NPF days, during which the measured air masses were notably influenced by either anthropogenic activities, biogenic emissions, or mixed ocean and continental sources. Overall, simulated NPF events were generally in good agreement with the corresponding measurements, enabling us to get further insights into NPF processes in the YRD region. Based on the simulations, we conclude that besides gas-phase sulphuric acid, biogenic organic compounds, particularly monoterpenes, play an essential role in condensational growth of newly formed clusters and probably also in the particle formation process through their low volatile oxidation products. Although some uncertainties remain in this modelling system, this method provides a possibility to better understand the NPF processes.

1 Introduction

Ambient aerosols affect human health adversely, degrade visibility, and play an important role in climate change through directly scattering/absorbing solar radiation or indirectly modifying microphysical properties of clouds (Eidels-Dubovoi, 2002; David-

ACPD
15, 27501–27538, 2015

son et al., 2005; Lohmann and Feichter, 2005; Myhre et al., 2013). Atmospheric new particle formation (NPF), characterized by a sharp increase in number concentration of nucleation-mode aerosol, has been observed under a wide variety of circumstances and has been shown as a significant source of atmospheric fine particles (O'Dowd et al., 2002; Kulmala and Kerminen, 2008; Gao et al., 2011; Guo et al., 2012, 2014; Wang et al., 2014). As the newly formed particles and their following growth may lead several-fold increases in aerosol number concentrations, atmospheric NPF could substantially contribute to the global CCN (Cloud condensation nuclei) budget and subsequent cooling effect (Lihavainen et al., 2003; Merikanto et al., 2009; Yu and Luo, 2009; Wang and Penner, 2009; Kerminen et al., 2012; Makkonen et al., 2012; Scott et al., 2015).

NPF has been extensively and intensively studied globally during the last two decades. It is well known that particle formation in the atmosphere is strongly dependent on the abundance of sulphuric acid (Weber et al., 1999; Kulmala et al., 2004b; Sipila et al., 2010). Meanwhile, other compounds in the atmosphere may also be responsible for NPF occurrence in different environments. Iodine-containing vapors were identified as the precursors for marine new particle formation (O'Dowd et al., 2002). Observations in Pittsburgh imply that ammonia could considerably enhance the atmospheric particle formation (Q. Zhang et al., 2004). In the boreal forest, oxidation products of monoterpenes together with sulphuric acid were very likely to lead to NPF (Schobesberger et al., 2013) and new findings indicate that organic amines (e.g. dimethylamine) can enhance water-sulphuric acid particle formation rates more than 1000-fold compared to ammonia (Almeida et al., 2013).

As one of the most economically invigorating and densely populated countries, China features simultaneous high aerosol loadings and NPF rates (S. Liu et al., 2008; Gao et al., 2011; Guo et al., 2012). Moreover, the condensational growth of nucleation-mode particles has been indicated as a plausible cause of regional haze events (Guo et al., 2014). Since 2000s, several field campaigns as well as long-term measurements have been conducted in several regions such as Beijing, the Pearl River Delta as well as the

ACPD
15, 27501–27538, 2015

Yangtze River Delta, showing high occurrence frequencies and formation rates across China (S. Liu et al., 2008; Gao et al., 2009; Yue et al., 2010; Herrmann et al., 2014; Qi et al., 2015; Xiao et al., 2015). However, modelling studies that provide a further insight into the processes of atmospheric aerosol formation, are still very limited in the China region. Numerical simulations of formation and growth processes require detailed and high time-resolving measurements of the relevant compounds, however, hardly can any field campaign or in-situ measurement station in China meet this requirement. The novel combination of an atmospheric chemical transport model and a zero-dimensional box model with detailed aerosol dynamics makes it possible to accomplish NPF studies without direct measurements of all specific chemical species. Here, we present a comprehensive modelling study on the occurrence of NPF events observed at the Station for Observing Regional Processes of the Earth System (SORPES) at Nanjing University in Nanjing, China (Ding et al., 2013a). This is the first attempt to integrate regional model, box model and in-situ measurements to investigate NPF events in China, enabling us to gain more insights into NPF mechanism in the YRD region.

2 Data and methodology

2.1 In-situ measurements

The SORPES site is located in the Xianlin campus of Nanjing University in the suburban area northeast of Nanjing, which is about 20 km east from the downtown area (118°57′10″ E, 32°7′14″ N, 40 m a.s.l. as shown in Fig. 1 in Ding et al., 2013a). This site, with few local emission sources around it, is generally upwind of downtown Nanjing and also downwind of the city clusters of the Yangtze River Delta. Hence it can be regarded as a regional background station (Ding et al., 2013a).

On-line and high time-resolving measurements of trace gases, aerosol characteristics, and relevant meteorological parameters have been conducted since the summer of 2011. Ozone (O_3), sulphur dioxide (SO_2), nitrogen monoxide (NO), nitrogen

ACPD
15, 27501–27538, 2015

dioxide (NO_2), total reactive nitrogen (NO_y), carbon monoxide (CO) and $PM_{2.5}$ (fine particulates less than 2.5 microns in aerodynamic diameter) are routinely measured by Thermo Instruments (TEI 49i, 43i, 42i, 42iY and 48i) and MARGA (Monitor for Aerosols and Gases in Ambient Air) (Ding et al., 2013a, b). The Differential Mobility Particle Sizer (DMPS) coupling a differential mobility analyzer with two different flow rates and a condensation particle counter are used to measure number distributions of atmospheric particles from 6 to 800 nm (Herrmann et al., 2014; Qi et al., 2015). More thorough information on the instruments at the SORPES site is elaborated in detail in Ding et al. (2013a, b).

2.2 Model description

2.2.1 MALTE-BOX model

MALTE is a one-dimension model comprising of boundary layer meteorology, biogenic emission of volatile organic compounds, gas-phase chemistry and aerosol dynamics in order to predict particle formation and growth processes under atmospheric conditions (Boy et al., 2006). Here, we apply the zero-dimensional version, namely, MALTE-BOX model, to simulate NPF events at the SORPES station. In the MALTE-BOX model, boundary layer meteorology and biogenic emission modules are switched off; instead, the biogenic and anthropogenic VOC emissions and their following dispersion are calculated by the regional chemical transport model WRF-Chem. Concentration of various organic compounds at the SORPES station predicted by WRF-Chem model are input to MALTE-BOX model every 10 min (Table 1 provides the compounds calculated by WRF-CHEM as input to MALTE-BOX). Likewise, measured concentrations of trace gases including CO, SO_2, NO, NO_2 and O_3, with the same temporal resolution, are also included as input fields. In addition to gas phase precursors, the inputs also include an initial particle number size distribution at 00:00 LT on each day, ambient temperature, relative humidity and the condensation sink of sulphuric acid (as defined in Sect. 2.3).

ACPD
15, 27501–27538, 2015

In the MALTE-BOX model, particles are assumed to be spherical. Fixed sectional approach with 40 size bins ranging from 1.4 to 2000 nm in diameter is used in the present study. The aerosol dynamics has all basic aerosol processes, including nucleation, condensation, coagulation, and deposition. The nucleation rates of newly-formed clusters are estimated by the kinetic nucleation theory of sulphuric acid (Sihto et al., 2006), which is related to the sulphuric acid concentration as follows:

$$J = k_1 \times [H_2SO_4]^2 \quad (1)$$

where k_1 is the kinetic coefficient that includes both the collision frequency and the probability of forming a stable cluster after the collision. Kinetic nucleation theory has been shown to provide good cluster formation rate in various environments including both clean continental area and polluted urban site (Wang et al., 2013b; Zhou et al., 2014). The nucleated particles were added to the first size bin in the model.

A set of sensitivity simulations were conducted to establish a suitable value for the nucleation coefficient k_1. After comparing the simulations and DMPS measurements, k_1 was set to 6.0×10^{-19} for 10 July and 22 August, and 2.2×10^{-16} for 22 June, respectively. These values were much smaller than those we commonly used in the simulations for NPF in the Boreal forest (Paasonen et al., 2010; Zhou et al., 2014). Such notable differences might imply that other molecules, like gaseous amines, air ions or currently unrecognized sources of low volatile vapors, are involved and play a crucial role in the particle formation process at this urban site. Moreover, being limited by the detectable size of the DMPS (what we can monitor are the particles larger than 6 nm in diameter), means that the observed formation process could be steered by the condensational growth of the smallest clusters to the detection limit.

We included relevant chemical reactions of the MCM (Master Chemical Mechanism) in this model, as described in Boy et al. (2013). Apart from sulphuric acid, about twenty low-volatility organic compounds (ELVOCs) and seven selected semi volatile organic compounds (SVOCs) are regarded as condensing vapors, following the simplified chemical mechanism presented by Ehn et al. (2014). Specifically, seven rep-

ACPD
15, 27501–27538, 2015

resentative SVOCs (MCM-nomenclature: C719OOH, LIMALOOH, C924OOH, NORLIMOOH, C811OOH, C818OOH and C819OOH) with vapor pressures estimated to range from 10^4 to 10^6 molecules cm^{-3} (using the group contribution method described by Nannoolal et al., 2008) and recently detected ELVOCs ($C_{10}O_{5-12}H_x$, $C_{10}NO_{5-13}H_x$ and $C_{20}O_{8-16}H_x$) with vapor pressures between 10 and 10^3 molecules cm^{-3} are introduced in the model.

2.2.2 WRF-Chem

The WRF-Chem version 3.6 was used here to estimate concentrations of various organic vapors from anthropogenic and biogenic emissions as there was no VOCs measurement at the SORPES site during the study period. WRF-Chem is an online three-dimensional, Eulerian chemical transport model that considers the complex physical and chemical processes, such as emission and deposition of pollutants, advection and diffusion, gaseous and aqueous chemical transformation, aerosol chemistry and dynamics (Grell et al., 2005). It is capable of simulating atmospheric chemistry on a regional scale and has been successfully applied in several of our previous studies (Huang et al., 2014, 2015). In this study, the model domain covered East China and its surrounding area, centering at 32.0° N, 119.0° E with a 20 km × 20 km grid resolution, as demonstrated in Fig. 1. There are 24 vertical layers from the ground level to the top pressure of 50 hPa, in which 10 layers are placed under 1 km to better resolve the boundary layer process. The 6 hourly Final operational global analysis (FNL) data with a 1° × 1° spatial resolution produced by the National Centers for Environmental Prediction (NCEP) was used as initial and boundary conditions of meteorological fields. The simulations were conducted for June to August 2013 when NPF events were frequently detected. During the simulation period, each run covered 60 h, in which the first 12 h were just for model spin-up and the last 48 h results were adopted for further analysis and box modeling. The outputs of chemical species from the previous run were used as the initial and boundary conditions for the following run. Key physical parameterization options for the WRF-Chem modelling are the Noah land surface scheme to describe

ACPD
15, 27501–27538, 2015

the land–atmosphere interactions (Ek et al., 2003), the Lin microphysics scheme (Lin et al., 1983) with the Grell cumulus parameterization to reproduce the cloud and precipitation processes (Grell and Devenyi, 2002), the YSU boundary layer scheme (Hong, 2010), and the RRTMG short- and long-wave radiation scheme (Mlawer et al., 1997).

Anthropogenic emissions from power plants, residential combustion, industrial processes, on-road mobile sources and agricultural activities were derived from the MEIC database (Multi-resolution Emission Inventory for China, see www.meicmodel.org). Emissions of major pollutants, such as carbon monoxide, sulphur dioxide, nitrogen oxides, ammonia and speciated VOCs are all included in this emission inventory database. MEGAN (Model of Emissions of Gases and Aerosols from Nature, version 2) module embedded in WRF-Chem is used to calculate biogenic emissions online (Guenther et al., 2006). It estimates the net emission rates of isoprene, monoterpene and other biogenic VOCs from terrestrial ecosystems into the above-canopy atmosphere. Gas-phase chemistry is explicitly represented by the model through the SAPRC photochemistry scheme (Carter, 1999), which includes 225 gas-phase reactions among 81 chemical species in the model. We mapped some predicted organic species in WRF-Chem to the MALTE-BOX following the correspondence denoted in Table 1. Regarding the monoterpenes (alpha-pinene, beta-pinene, camphene, myrcene, carene and limonene) used in MALTE-BOX chemistry (details in Boy et al., 2013), the distribution was performed equally because no VOC-measurements at the SORPES station were available.

2.3 Data analysis

The calculations of particle growth and formation rates are conducted following the procedures outlined by Kulmala et al. (2012). The formation rate is obtained from the following equation:

$$J_{\mathrm{dp}} = \frac{\mathrm{d}N_{\mathrm{dp}}}{\mathrm{d}t} + \mathrm{Coag}S_{\mathrm{dp}} \times \frac{\mathrm{GR}}{D_{\mathrm{dp}}} N_{\mathrm{dp}} + S_{\mathrm{losses}} \quad (2)$$

ACPD
15, 27501–27538, 2015

where J_{dp} is the particle formation rate of diameter dp, the first term on the right side is the time evolution of the particle number concentration with size dp. CoagS_{dp} is the coagulation loss. The second term describes the growth out of the considered size, where GR is the observed growth rate. The last term S_{losses} represents additional losses, which were not considered in this study.

The growth rate of particles during the NPF events can be expressed as

$$GR_{dp} = \frac{d_{p1} - d_{p2}}{t_1 - t_2} \quad (3)$$

where d_{p1} and d_{p2} are the representative of the diameter of nucleated particles at the times t_1 and t_2, respectively. For calculation, d_{p1} and d_{p2} is then defined as the central size of each bin and t_1 and t_2 are the moments when the concentration of this size bin peaks.

The condensation sink determines how rapidly condensable vapor molecules will condense onto pre-existing aerosols. It can be derived by DMPS-measured particle number size distribution according to the following method (Kulmala et al., 2001).

$$CS = 4\pi D \sum_{dp'} \beta_{m,dp'} dp' N_{dp'} \quad (4)$$

where D is the diffusion coefficient of the condensing vapor, β_m is a transition-regime correction, dp′ is the discrete diameter and $N_{dp'}$ is the particle number concentration in respective size bin.

3 Results and discussions

This chapter is divided into two parts. The first subsection provides discussion of measured particle size distributions on three typical NPF days. Air mass transport pathways and parameters that favor the formation of new particles at the SORPES site will be

ACPD
15, 27501–27538, 2015

investigated. The second subsection focuses on the numerical simulation of observed NPF events. A further detailed analysis of particle formation and following growth will be presented.

3.1 Observations and data analysis

Summer marks the season with frequent NPF events at the SORPES site, especially in the year of 2013 (Qi et al., 2015). From June to August 2013, 50 NPF events were detected during the 76 day measurement period when DMPS functioned normally, resulting in the particle formation probability of 66 %. Among the observed NPF events, three representative cases were identified according to the retroplumes calculated based on Lagrangian dispersion model HYSPLIT (Hybrid Single Particle Lagrangian Integrated Trajectory Model) following the method developed by Ding et al. (2013c). These selected NPF days are 22 June, 10 July and 22 August 2013, when the site was dominantly influenced by the air masses from the YRD region, South China, and mixed ocean and continental areas, respectively (Fig. 2).

On 22 June 2013, a clear banana-shaped particle size distribution was captured by the DMPS in the morning (09:00–11:00 LT, Fig. 3). According to the DMPS observations, the number concentration of particles with diameter ranging from 6 to 30 nm reached up to over 500 000 # cm^{-3} around 10:30 LT. The formation rate of 6 nm particles, namely J_6 calculated following Eq. (2), was 7.6 $cm^{-3}\,s^{-1}$. It was generally comparable to those typically observed elsewhere in China, for instance, 0.97–10.2 $cm^{-3}\,s^{-1}$ in Hong Kong ($J_{5.5}$) (Guo et al., 2012). The diurnal variations of measured number size distribution and relevant trace gases are demonstrated in Fig. 3. This NPF event featured a large background particle loading with $PM_{2.5}$ mass concentration exceeding 50 $\mu g\,m^{-3}$ because the air mass was lingering over city clusters in the YRD region before approaching the SORPES station, as shown in Fig. 2a. Dense particle emissions from the rapidly urbanized and industrialized YRD region (Fig. 2e) correspond to a high condensation sink of $4.2 \times 10^{-2}\,s^{-1}$, close to those typically observed in other urban ar-

ACPD
15, 27501–27538, 2015

eas in China (Gao et al., 2012; Xiao et al., 2015). For the same reason, influenced by the emissions in the YRD region (Fig. 2d), SO_2 concentration was observed to be 20–30 ppb, considerably higher than the normally observed level at the site, which is less than 10 ppb during summertime (Ding et al., 2013a). Along with the active photochemistry and high concentration of O_3, rapid oxidation of SO_2 and accumulation of gaseous sulphuric acid are expected, leading to the onset of NPF despite the high level of condensation sink. The subsequent growth was fast, with a GR_{6-30} (growth rate from 6 to 30 nm) of 12.6 nm h^{-1}. Accumulating sulphuric acid with increasing ozone concentration might be a contributor. In addition, the presence of aromatic-related oxidation products from residential and industrial combustion in the YRD region could also substantially enhance particle formation and subsequent growth by absorption or heterogeneous reactions (R. Y. Zhang et al., 2004; Y. Liu et al., 2008).

On 10 July when the air masses mostly came from the densely wooded area in South China, NPF showed much lower new particle formation rates than on 22 June, yet a slightly faster particle growth rate (Table 2). Previous investigations have revealed that overall GR is correlated with the rate of terpene reactions with atmospheric photochemical oxidants, highlighting the importance of biogenic VOCs in the particle growth process (e.g. Boy et al., 2003; Kulmala et al., 2004a). During the QUEST (Quantification of Aerosol Nucleation in the European Boundary Layer) field campaign in Hyytiälä, Finland, recorded particle growth rates during NPF events correlated notably with gas-phase monoterpene concentrations, indicating that the oxidation products from biogenic VOCs may dominate particle growth (Laaksonen et al., 2008; Yli-Juuti et al., 2011). The positive correlation between freshly formed particle growth rates and monoterpenes and their oxidation rates by ozone was also verified in Hong Kong, China (Guo et al., 2012). Figure 2f presents the spatial distribution of monoterpene emission rates during summertime across China calculated by the MEGAN model (Li et al., 2012). It is obvious that monoterpene emission is overwhelmingly intensive in South China, which is covered by large areas of broadleaf forests and shrubs. It is plausible that air masses passed over biogenic VOC-rich regions were saturated with sufficiently

ACPD
15, 27501–27538, 2015

low volatile oxidation products, which enhanced the observed particle growth. The simulation results from the WRF-Chem model supported this view. Modelled isoprene and terpene concentrations were 1.2 and 0.15 ppb at the SORPES site during NPF on 10 July, 150 and 50 % higher than the corresponding values on 22 June. Besides, lower pre-existing particle loading is another cause of faster growth due to less particle surface area for condensable vapors.

Another NPF event, characterized by mixed marine and continental source regions, occurred on 22 August. Because of relatively clean air from the ocean and high wind speed of around 8 $m\,s^{-1}$, $PM_{2.5}$ and SO_2 concentrations were unusually low, only 11.0 $\mu g\,m^{-3}$ and 2.8 ppb when NPF event took place. Accordingly, the condensation sink fell down to $10^{-3}\,s^{-1}$. Existing measurements and analysis concluded that the main obstacle for the initial onset of new particle formation at the SORPES site is condensation sink, since the SO_2 concentration is always high and there tends to be enough solar radiation as well (Herrmann et al., 2014). So, even though the SO_2 concentration was pretty low during that day, strong radiation level together with a fairly small condensation sink could have jointly triggered the onset of this NPF event. The nuclei growth rate, GR_{6-30}, was estimated to be 15.7 $nm\,h^{-1}$. On one hand, humid air mass transported from the ocean might have favored the particle growth. As displayed in Fig. 3, the measured relative humidity (RH) was over 80 % when the NPF began. On the other hand, the sampling site was also partly influenced by the air masses from the YRD region (Fig. 2c), which means that anthropogenic VOCs and oxidation products with low volatility might also exert a notable impact on particle growth.

3.2 Simulations of NPF events

To shed further light on NPF processes at the SORPES station, comprehensive simulations were performed by combining WRF-Chem regional atmospheric transport model and the MALTE-BOX model. Measurements of meteorological fields, trace gases and aerosol characteristics from the SORPES station are input to the box model. In the meantime, input also includes the concentrations of gaseous organic compounds from

ACPD
15, 27501–27538, 2015

the WRF-Chem regional model (see Table 1). The simulations were conducted for the aforementioned three NPF days.

3.2.1 Evaluation of simulations by WRF-Chem model

Meteorological conditions play an important part in transport, diffusion, and chemical reactions in the atmosphere. Simulated hourly 2 m temperature and 10 m wind speed were evaluated using hourly temperature and relative humidity observations at the SORPES station. Statistical analyses of model performance for the three NPF days are listed in Table 3, including mean bias (MB) and root mean square error (RMSE). Generally, the model reproduced well the observed 2 m temperature and 10 m wind. As mentioned, modelled VOC concentrations, which are vital for NPF simulation, are included as an input field in the MALTE-BOX model. Although there was no VOC measurement during the summer of 2013, the SORPES site and the Environmental Monitoring Center of Jiangsu Province (118°47′ E, 32°4′ N) were equipped with GC/MS (gas chromatography/mass spectrometry) in the summer of 2014. In order to evaluate model's performance in simulating VOC concentrations, we conducted another WRF-Chem run for the August of 2014 and then compared the model results with corresponding observations. The comparison of alkene, aromatic and isoprene concentrations in Fig. 4a–c illustrates that WRF-Chem succeeds, on average, to generally reproduce VOCs originating from both anthropogenic and biogenic sources. In term of the biogenic terpenes, whose oxidation products have low vapor pressures similar to sulphuric acid and condense onto aerosol surfaces, the spatial patterns in the morning of the aforementioned three NPF days showed great differences (Fig. 4d–f). During the first and third NPF cases, prevailing easterly winds did not bring much biogenic VOC since biogenic emissions are most intensive in the southern part of China. By contrast, on 10 July when southwesterly winds dominated, the modelled terpene concentrations at the SORPES station were almost two times those in the other two NPF days.

ACPD
15, 27501–27538, 2015

3.2.2 MALTE-BOX simulations

Figure 5 shows the variations of modelled particle number size distributions during the 3 NPF days. The model system does reproduce the occurrence of these three NPF events although they were under distinct meteorological conditions and affected by entirely different potential source regions. On 22 June when measured air masses originated from the urbanized YRD region, the calculated onset of activation of freshly formed cluster to grow above the 6 nm line appeared around 08:30 LT. According to the diurnal pattern of simulated concentrations of gaseous compounds illustrated in Fig. 6, the OH radical level increased rapidly from 1×10^5 to 3×10^6 # cm^{-3} just after sunrise, promoting the gaseous oxidation of SO_2 in the atmosphere and subsequent accumulation of sulphuric acid. Simultaneously, the pre-existing particle concentration dropped down due to the boundary layer evolution (Fig. 3). The continuously growing sulphuric acid concentration and decreasing condensation sink jointly led to this fast NPF event. During the second NPF case, the OH radical concentration was mostly less than 1×10^6 # cm^{-3}. The production of sulphuric acid was expected to be relatively slow due to the simultaneous lower concentrations of both SO_2 and OH radical. As demonstrated in Fig. 6, the sulphuric acid was approximately 3×10^5 # cm^{-3} just when the NPF started, about one-tenth and one-seventh of the corresponding values on 22 June and 22 August, respectively. Nonetheless, prevailing southwesterly winds brought along terpene-rich air masses. Some of the terpenes, such as alpha-pinene and limonene, feature significantly high yields of ELVOCs as well as SVOCs while reacting with ozone or OH radicals (Ehn et al., 2014; Jokinen et al., 2015). Such dense low volatile oxidation products enhance condensational growth of newly formed particles. Unlike during the first two NPF cases, the level of pre-existing particles was unusually low during the third event because a strong wind from the ocean swept over East China. The clean air mass reduced the condensation sink to 10^{-3} s^{-1} (Table 2), much lower than the values typically observed at the SORPES site before (Herrmann et al., 2014). Consequently, sulphuric acid accumulated remarkably in the gas phase due to little condensational

ACPD
15, 27501–27538, 2015

loss even though SO_2 concentrations were pretty low. The third NPF case reaffirms the previous conclusion that condensation sink is the most important obstacle for NPF at this experimental site (Herrmann et al., 2014).

Though the model succeeded in the prediction of DMPS-measured NPF occurrence, the simulated activation of NPF was about one hour later than the observations. Considering the number concentration in the size range 6–10 nm (N_{6-10}) as the newly formed particles, model shows a distinct underestimation at the beginning of the NPF events (Fig. 5). As mentioned in Sect. 2, we assumed the kinetic mechanism in the MALTE-BOX, in which two sulphuric acid molecules collide with each other to form a cluster as in the kinetic gas theory. Nonetheless, chamber and in-situ experiments speculated that monoterpene oxidation products could cluster directly with a single sulphuric acid molecule under ambient conditions and that the interaction between organic and sulphuric acids likely leads to a reduced nucleation barrier (R. Y. Zhang et al., 2004; Schobesberger et al., 2013). Furthermore, according to the simulation, the production of ELVOCs and SVOCs was mainly initialized by the reactions between monoterpene and ozone. It has been recognized that NPF events tend to be strongly associated with the monoterpene oxidation products by ozone in both remote and urban environments (Laaksonen et al., 2008; Guo et al., 2012). Thus, there was a good chance that the ELVOCs played an important part in the NPF processes considered here. As presented in Fig. 6, a considerable amount of ELVOCs accumulated before modelled NPF occurred, as well as during the observed NPF events. The time shifts of the starting times is consistent with the hypothesis that organic vapors may play a key role in the particle formation process (Paasonen et al., 2009; Metzger et al., 2010). Figure 7a shows the dependence of measurement-derived nucleation rates (J_6) on modelled gaseous sulphuric acid and ELVOC concentrations. 6 nm nucleation rates, even under the same sulphuric acid concentration, were substantially enhanced by the presence of ELVOCs. It is noteworthy that formation rates of 6 nm particles, not nucleation rates, are available here due to the limitation of instruments. It is hard to identify which process is mostly promoted by ELVOCs, either the particle formation or the early

ACPD
15, 27501–27538, 2015

condensational growth. Metzger et al. (2010) attempted to disentangle the influence of organic oxidation products in particle formation and suggested an overall dependency on the formation rate of H_2SO_4 and organic oxidation products with the lowest volatility (NucOrg) as listed below.

$$J_{1.5} = k \times [H_2SO_4]^{1.0}[\mathrm{NucOrg}]^{0.8} \quad (5)$$

where, $J_{1.5}$ is nucleation rate of 1.5 nm cluster; k represents prefactor which recommended to be $7.2 \pm 1.4 \times 10^{-13}$ $\mathrm{cm^3\,s^{-1}}$ in Metzger et al. (2010); $[H_2SO_4]$ and [NucOrg] refer to the concentration of sulphuric acid and low volatile organic oxidation products that can participate in the particle formation process, respectively. By assuming that NucOrg is part of the ELVOCs in the present work, we examined the relationships between measured particle formation rate with $[H_2SO_4]^{1.0}[\mathrm{ELVOCs}]^{0.8}$ and compared it with $[H_2SO_4]^2$ in Fig. 7b and c. The better representation and correlation of the latter provides further evidence for an involvement of ELVOCs in NPF process or the very initial growth of the newly nucleated clusters.

In terms of the condensational growth of freshly-formed particles, ambient low-volatility compounds are predominant contributors, in particular, semi-volatile and possibly non-volatile organic matters generating from a complex series of photochemical reactions (Kroll and Seinfeld, 2008). In the present work, the model notably underestimates the nuclei condensational growth (GR_{6-30}) for Case 1 and Case 3 compared with the corresponding observations, whereas the observation and simulation were comparable for the Case 2 (Table 2). These differences could partly be due to the fact that here we only took oxidation products for certain selected organic compounds into account as sources of condensable vapors. When the experimental site was substantially influenced by intensive industrial activities and vehicle emissions from the YRD region in Case 1 and Case 3, reactive uptake and condensable secondary organic products from anthropogenic VOCs, which actually do accelerate particle growth (R. Y. Zhang et al., 2004; Kroll et al., 2005; Volkamer et al., 2006), were partly missing in the present model. This causes the underestimation of particle growth rates. Regarding the im-

ACPD
15, 27501–27538, 2015

pacts of biogenic VOCs, we found that ELVOCs and SVOCs remarkably contributed to particle condensational growth. According to the simulation, ELVOCs and SVOCs were responsible for 70–80 % of the overall modelled growth rate during NPF Case 1 and Case 3. The contribution was even higher than 95 % in the second case when the terpene-rich air mass approached at the experimental site.

3.2.3 Model uncertainties

The comprehensive modelling study on the observed new particle formation makes it possible to better understand NPF processes at the SORPES station. However, there still lie many uncertainties in this modelling system, which need to be improved in future work. Given the expensive computational cost, reactions of VOCs are represented by the lumped mechanism in the regional-scale WRF-Chem model. Relevant parameters cannot be precisely determined for one lumped class, while the MALTE-BOX model provides accurate information for each specific organic compound. The gaps between the two models concerning VOC classification would introduce considerable uncertainties. Moreover, in the MALTE-BOX model, sulphuric acid tends to be underpredicted, which was demonstrated in both polluted urban environment and clean rural environment (Wang et al., 2013a; Zhou et al., 2014, 2015). There are multiple reasons behind the systematic underestimation. It has been shown by field measurements, laboratory experiments and numeric simulation that Crigee Intermediates (CIs) or other derivatives are capable of accelerating the oxidation of SO_2 into SO_3 (Hatakeyama and Akimoto, 1994; Kurten et al., 2011; Boy et al., 2013). These reactions have been incorporated in the MALTE-BOX model but would need further investigations concerning the reactions rates and other important reaction parameters (e.g. thermal lifetimes of CIs, pressure dependency, etc.). In addition, owing to the far incomplete knowledge of HONO sources, in particular during daytime, it was not yet possible to simulate realistic HONO levels using current models (Elshorbany et al., 2014; Czader et al., 2015). The lack of HONO measurement input to the model might also result in an underestimation of sulphuric acid, especially with dramatically increasing traffic emissions during

ACPD
15, 27501–27538, 2015

the rush hours (Wang et al., 2013b). For instance, in the first case, the air masses were carrying on more characteristic from the emissions-intensive YRD region, the sulphuric acid concentrations and particle formation rates are more likely to be under-predicted. Last but not least, we adopted a mandatory value for the kinetic coefficient, which includes the probability that a collision of two molecules results in the formation of a stable critical cluster, as well as all other important details concerning the particle formation process such as temperature and humidity. This condition-dependent coefficient needs to be resolved in further modelling work on the basis of more in-situ and laboratory experiments.

4 Conclusions

This study combines the regional chemical transport model and box model to investigate atmospheric new particle formation and its subsequent nuclei condensational growth at the SORPES site in Nanjing, China. This combination makes it possible to simulate chemical and aerosol dynamical processes. Three NPF cases, during which the experimental site was influenced by entirely different potential source regions, were successfully reproduced by the modelling system. When the site was predominately influenced by air masses from city clusters in the YRD on 22 June 2013, despite a high condensation sink, the NPF event featured fast nucleation rate due to the continuously accumulating sulphuric acid. Under the circumstance that biogenic VOC-rich air masses dominated, rapid growth of freshly formed particle was detected on 10 July 2013, which was attributed to the low-volatility oxidation products of terpenes. Air masses from marine origin could lead to the relatively low condensation sink on 22 August 2013, thereby facilitating the occurrence of NPF event. On the basis of measurements and the corresponding modelling, we infer the controlling factors of the selected three NPF events, and these were mostly associated with sulphuric acid accumulation and low condensation sink. The comparison with the observations suggested that low-volatility organic compounds played a substantial role in the initial condensational

ACPD
15, 27501–27538, 2015

growth of the particles, and probably also in the particle formation process. In addition, anthropogenic VOCs and the following photochemical oxidation produce a considerable amount of condensable compounds, exerting a significant impact on particle growth in the emission-intensive YRD region. Although some inadequacies still remain, such as the inclusion of anthropogenic nonvolatile organic compounds as condensable vapors, the comprehensive modelling work provides a better insight of NPF processes.

Acknowledgements. This work was supported by the National Natural Science Foundation of China (D0512/41305123, D0512/4142200036, D03/41321062 and D0510/41505109). Part of this work was supported by the Jiangsu Provincial Science Fund for Distinguished Young Scholars awarded to A. J. Ding (No. BK20140021) and by the Academy of Finland projects (1118615, 139656) and the European Commission via ERC Advanced Grant ATM-NUCLE. We also thank the financial support from Helsinki University Centre of Environment (HENVI).

References

Almeida, J., Schobesberger, S., Kurten, A., Ortega, I. K., Kupiainen-Maatta, O., Praplan, A. P., Adamov, A., Amorim, A., Bianchi, F., Breitenlechner, M., David, A., Dommen, J., Donahue, N. M., Downard, A., Dunne, E., Duplissy, J., Ehrhart, S., Flagan, R. C., Franchin, A., Guida, R., Hakala, J., Hansel, A., Heinritzi, M., Henschel, H., Jokinen, T., Junninen, H., Kajos, M., Kangasluoma, J., Keskinen, H., Kupc, A., Kurten, T., Kvashin, A. N., Laaksonen, A., Lehtipalo, K., Leiminger, M., Leppa, J., Loukonen, V., Makhmutov, V., Mathot, S., McGrath, M. J., Nieminen, T., Olenius, T., Onnela, A., Petaja, T., Riccobono, F., Riipinen, I., Rissanen, M., Rondo, L., Ruuskanen, T., Santos, F. D., Sarnela, N., Schallhart, S., Schnitzhofer, R., Seinfeld, J. H., Simon, M., Sipila, M., Stozhkov, Y., Stratmann, F., Tome, A., Trostl, J., Tsagkogeorgas, G., Vaattovaara, P., Viisanen, Y., Virtanen, A., Vrtala, A., Wagner, P. E., Weingartner, E., Wex, H., Williamson, C., Wimmer, D., Ye, P. L., Yli-Juuti, T., Carslaw, K. S., Kulmala, M., Curtius, J., Baltensperger, U., Worsnop, D. R., Vehkamaki, H., and Kirkby, J.: Molecular understanding of sulphuric acid-amine particle nucleation in the atmosphere, Nature, 502, 359–363, doi:10.1038/Nature12663, 2013.

ACPD
15, 27501–27538, 2015

Boy, M., Rannik, U., Lehtinen, K. E. J., Tarvainen, V., Hakola, H., and Kulmala, M.: Nucleation events in the continental boundary layer: Long-term statistical analyses of aerosol relevant characteristics, J. Geophys. Res.-Atmos., 108, 4667, doi:10.1029/2003jd003838, 2003.
Boy, M., Hellmuth, O., Korhonen, H., Nilsson, E. D., ReVelle, D., Turnipseed, A., Arnold, F., and Kulmala, M.: MALTE – model to predict new aerosol formation in the lower troposphere, Atmos. Chem. Phys., 6, 4499–4517, doi:10.5194/acp-6-4499-2006, 2006.
Boy, M., Mogensen, D., Smolander, S., Zhou, L., Nieminen, T., Paasonen, P., Plass-Dülmer, C., Sipilä, M., Petäjä, T., Mauldin, L., Berresheim, H., and Kulmala, M.: Oxidation of SO_2 by stabilized Criegee intermediate (sCI) radicals as a crucial source for atmospheric sulfuric acid concentrations, Atmos. Chem. Phys., 13, 3865–3879, doi:10.5194/acp-13-3865-2013, 2013.
Carter, W. P. L.: Documentation of the SAPRC-99 Chemical Mechanism for VOC Reactivity Assessment, open file rep., University of California, Riverside, CA, USA, 446 pp., 1999.
Czader, B. H., Choi, Y., Li, X., Alvarez, S., and Lefer, B.: Impact of updated traffic emissions on HONO mixing ratios simulated for urban site in Houston, Texas, Atmos. Chem. Phys., 15, 1253–1263, doi:10.5194/acp-15-1253-2015, 2015.
Davidson, C. I., Phalen, R. F., and Solomon, P. A.: Airborne particulate matter and human health: a review, Aerosol Sci. Tech., 39, 737–749, doi:10.1080/02786820500191348, 2005.
Ding, A. J., Fu, C. B., Yang, X. Q., Sun, J. N., Zheng, L. F., Xie, Y. N., Herrmann, E., Nie, W., Petäjä, T., Kerminen, V.-M., and Kulmala, M.: Ozone and fine particle in the western Yangtze River Delta: an overview of 1 yr data at the SORPES station, Atmos. Chem. Phys., 13, 5813–5830, doi:10.5194/acp-13-5813-2013, 2013a.
Ding, A. J., Fu, C. B., Yang, X. Q., Sun, J. N., Petäjä, T., Kerminen, V.-M., Wang, T., Xie, Y., Herrmann, E., Zheng, L. F., Nie, W., Liu, Q., Wei, X. L., and Kulmala, M.: Intense atmospheric pollution modifies weather: a case of mixed biomass burning with fossil fuel combustion pollution in eastern China, Atmos. Chem. Phys., 13, 10545–10554, doi:10.5194/acp-13-10545-2013, 2013b.
Ehn, M., Thornton, J. A., Kleist, E., Sipila, M., Junninen, H., Pullinen, I., Springer, M., Rubach, F., Tillmann, R., Lee, B., Lopez-Hilfiker, F., Andres, S., Acir, I. H., Rissanen, M., Jokinen, T., Schobesberger, S., Kangasluoma, J., Kontkanen, J., Nieminen, T., Kurten, T., Nielsen, L. B., Jorgensen, S., Kjaergaard, H. G., Canagaratna, M., Dal Maso, M., Berndt, T., Petaja, T., Wahner, A., Kerminen, V. M., Kulmala, M., Worsnop, D. R., Wildt, J., and

ACPD
15, 27501–27538, 2015

Mentel, T. F.: A large source of low-volatility secondary organic aerosol, Nature, 506, 476–479, doi:10.1038/Nature13032, 2014.
Eidels-Dubovoi, S.: Aerosol impacts on visible light extinction in the atmosphere of Mexico City, Sci. Total Environ., 287, 213–220, doi:10.1016/S0048-9697(01)00983-4, 2002.
Ek, M. B., Mitchell, K. E., Lin, Y., Rogers, E., Grunmann, P., Koren, V., Gayno, G., and Tarpley, J. D.: Implementation of Noah land surface model advances in the National Centers for Environmental Prediction operational mesoscale Eta model, J. Geophys. Res.-Atmos., 108, 8851, doi:10.1029/2002jd003296, 2003.
Elshorbany, Y. F., Crutzen, P. J., Steil, B., Pozzer, A., Tost, H., and Lelieveld, J.: Global and regional impacts of HONO on the chemical composition of clouds and aerosols, Atmos. Chem. Phys., 14, 1167–1184, doi:10.5194/acp-14-1167-2014, 2014.
Gao, J., Wang, T., Zhou, X. H., Wu, W. S., and Wang, W. X.: Measurement of aerosol number size distributions in the Yangtze River delta in China: formation and growth of particles under polluted conditions, Atmos. Environ., 43, 829–836, doi:10.1016/j.atmosenv.2008.10.046, 2009.
Gao, J., Chai, F. H., Wang, T., and Wang, W. X.: Particle number size distribution and new particle formation (NPF) in Lanzhou, Western China, Particuology, 9, 611–618, doi:10.1016/j.partic.2011.06.008, 2011.
Gao, J., Chai, F. H., Wang, T., Wang, S. L., and Wang, W. X.: Particle number size distribution and new particle formation: new characteristics during the special pollution control period in Beijing, J. Environ. Sci.-China, 24, 14–21, doi:10.1016/S1001-0742(11)60725-0, 2012.
Grell, G. A. and Devenyi, D.: A generalized approach to parameterizing convection combining ensemble and data assimilation techniques, Geophys. Res. Lett., 29, 1693, doi:10.1029/2002gl015311, 2002.
Grell, G. A., Peckham, S. E., Schmitz, R., McKeen, S. A., Frost, G., Skamarock, W. C., and Eder, B.: Fully coupled "online" chemistry within the WRF model, Atmos. Environ., 39, 6957–6975, 2005.
Guenther, A., Karl, T., Harley, P., Wiedinmyer, C., Palmer, P. I., and Geron, C.: Estimates of global terrestrial isoprene emissions using MEGAN (Model of Emissions of Gases and Aerosols from Nature), Atmos. Chem. Phys., 6, 3181–3210, doi:10.5194/acp-6-3181-2006, 2006.

ACPD
15, 27501–27538, 2015

Guo, H., Wang, D. W., Cheung, K., Ling, Z. H., Chan, C. K., and Yao, X. H.: Observation of aerosol size distribution and new particle formation at a mountain site in subtropical Hong Kong, Atmos. Chem. Phys., 12, 9923–9939, doi:10.5194/acp-12-9923-2012, 2012.
Guo, S., Hu, M., Zamora, M. L., Peng, J. F., Shang, D. J., Zheng, J., Du, Z. F., Wu, Z., Shao, M., Zeng, L. M., Molina, M. J., and Zhang, R. Y.: Elucidating severe urban haze formation in China, P. Natl. Acad. Sci. USA, 111, 17373–17378, doi:10.1073/pnas.1419604111, 2014.
Hatakeyama, S. and Akimoto, H.: Reactions of Criegee Intermediates in the Gas-Phase, Res. Chem. Intermediat., 20, 503–524, doi:10.1163/156856794x00432, 1994.
Herrmann, E., Ding, A. J., Kerminen, V.-M., Petäjä, T., Yang, X. Q., Sun, J. N., Qi, X. M., Manninen, H., Hakala, J., Nieminen, T., Aalto, P. P., Kulmala, M., and Fu, C. B.: Aerosols and nucleation in eastern China: first insights from the new SORPES-NJU station, Atmos. Chem. Phys., 14, 2169–2183, doi:10.5194/acp-14-2169-2014, 2014.
Hong, S. Y.: A new stable boundary-layer mixing scheme and its impact on the simulated East Asian summer monsoon, Q. J. Roy. Meteor. Soc., 136, 1481–1496, doi:10.1002/Qj.665, 2010.
Huang, X., Song, Y., Zhao, C., Li, M. M., Zhu, T., Zhang, Q., and Zhang, X. Y.: Pathways of sulfate enhancement by natural and anthropogenic mineral aerosols in China, J. Geophys. Res.-Atmos., 119, 14165–14179, doi:10.1002/2014jd022301, 2014.
Huang, X., Song, Y., Zhao, C., Cai, X. H., Zhang, H. S., and Zhu, T.: Direct Radiative Effect by Multicomponent Aerosol over China, J. Climate, 28, 3472–3495, doi:10.1175/Jcli-D-14-00365.1, 2015.
Jokinen, T., Berndt, T., Makkonen, R., Kerminen, V. M., Junninen, H., Paasonen, P., Stratmann, F., Herrmann, H., Guenther, A. B., Worsnop, D. R., Kulmala, M., Ehn, M., and Sipila, M.: Production of extremely low volatile organic compounds from biogenic emissions: Measured yields and atmospheric implications, P. Natl. Acad. Sci. USA, 112, 7123–7128, doi:10.1073/pnas.1423977112, 2015.
Kerminen, V.-M., Paramonov, M., Anttila, T., Riipinen, I., Fountoukis, C., Korhonen, H., Asmi, E., Laakso, L., Lihavainen, H., Swietlicki, E., Svenningsson, B., Asmi, A., Pandis, S. N., Kulmala, M., and Petäjä, T.: Cloud condensation nuclei production associated with atmospheric nucleation: a synthesis based on existing literature and new results, Atmos. Chem. Phys., 12, 12037–12059, doi:10.5194/acp-12-12037-2012, 2012.

ACPD
15, 27501–27538, 2015

Kroll, J. H. and Seinfeld, J. H.: Chemistry of secondary organic aerosol: formation and evolution of low-volatility organics in the atmosphere, Atmos. Environ., 42, 3593–3624, doi:10.1016/j.atmosenv.2008.01.003, 2008.

Kroll, J. H., Ng, N. L., Murphy, S. M., Varutbangkul, V., Flagan, R. C., and Seinfeld, J. H.: Chamber studies of secondary organic aerosol growth by reactive uptake of simple carbonyl compounds, J. Geophys. Res.-Atmos., 110, D23207, doi:10.1029/2005jd006004, 2005.

Kulmala, M. and Kerminen, V. M.: On the formation and growth of atmospheric nanoparticles, Atmos. Res., 90, 132–150, doi:10.1016/j.atmosres.2008.01.005, 2008.

Kulmala, M., Dal Maso, M., Makela, J. M., Pirjola, L., Vakeva, M., Aalto, P., Miikkulainen, P., Hameri, K., and O'Dowd, C. D.: On the formation, growth and composition of nucleation mode particles, Tellus B, 53, 479–490, doi:10.1034/j.1600-0889.2001.530411.x, 2001.

Kulmala, M., Suni, T., Lehtinen, K. E. J., Dal Maso, M., Boy, M., Reissell, A., Rannik, Ü., Aalto, P., Keronen, P., Hakola, H., Bäck, J., Hoffmann, T., Vesala, T., and Hari, P.: A new feedback mechanism linking forests, aerosols, and climate, Atmos. Chem. Phys., 4, 557–562, doi:10.5194/acp-4-557-2004, 2004a.

Kulmala, M., Vehkamaki, H., Petaja, T., Dal Maso, M., Lauri, A., Kerminen, V. M., Birmili, W., and McMurry, P. H.: Formation and growth rates of ultrafine atmospheric particles: a review of observations, J. Aerosol Sci., 35, 143–176, doi:10.1016/j.jaerosci.2003.10.003, 2004b.

Kulmala, M., Petaja, T., Nieminen, T., Sipila, M., Manninen, H. E., Lehtipalo, K., Dal Maso, M., Aalto, P. P., Junninen, H., Paasonen, P., Riipinen, I., Lehtinen, K. E. J., Laaksonen, A., and Kerminen, V. M.: Measurement of the nucleation of atmospheric aerosol particles, Nat. Protoc., 7, 1651–1667, doi:10.1038/nprot.2012.091, 2012.

Kurten, T., Lane, J. R., Jorgensen, S., and Kjaergaard, H. G.: A computational study of the oxidation of SO_2 to SO_3 by gas-phase organic oxidants, J. Phys. Chem. A, 115, 8669–8681, doi:10.1021/Jp203907d, 2011.

Laaksonen, A., Kulmala, M., O'Dowd, C. D., Joutsensaari, J., Vaattovaara, P., Mikkonen, S., Lehtinen, K. E. J., Sogacheva, L., Dal Maso, M., Aalto, P., Petäjä, T., Sogachev, A., Yoon, Y. J., Lihavainen, H., Nilsson, D., Facchini, M. C., Cavalli, F., Fuzzi, S., Hoffmann, T., Arnold, F., Hanke, M., Sellegri, K., Umann, B., Junkermann, W., Coe, H., Allan, J. D., Alfarra, M. R., Worsnop, D. R., Riekkola, M. -L., Hyötyläinen, T., and Viisanen, Y.: The role of VOC oxidation products in continental new particle formation, Atmos. Chem. Phys., 8, 2657–2665, doi:10.5194/acp-8-2657-2008, 2008.

ACPD
15, 27501–27538, 2015

Li, M., Huang, X., Li, J., and Song, Y.: Estimation of biogenic volatile organic compound (BVOC) emissions from the terrestrial ecosystem in China using real-time remote sensing data, Atmos. Chem. Phys. Discuss., 12, 6551–6592, doi:10.5194/acpd-12-6551-2012, 2012.

Lihavainen, H., Kerminen, V. M., Komppula, M., Hatakka, J., Aaltonen, V., Kulmala, M., and Viisanen, Y.: Production of "potential" cloud condensation nuclei associated with atmospheric new-particle formation in northern Finland, J. Geophys. Res.-Atmos., 108, 4782, doi:10.1029/2003jd003887, 2003.

Lin, Y. L., Farley, R. D., and Orville, H. D.: Bulk parameterization of the snow field in a cloud model, J. Clim. Appl. Meteorol., 22, 1065–1092, doi:10.1175/1520-0450(1983)022<1065:Bpotsf>2.0.Co;2, 1983.

Liu, S., Hu, M., Wu, Z. J., Wehner, B., Wiedensohler, A., and Cheng, Y. F.: Aerosol number size distribution and new particle formation at a rural/coastal site in Pearl River Delta (PRD) of China, Atmos. Environ., 42, 6275–6283, doi:10.1016/j.atmosenv.2008.01.063, 2008.

Liu, Y., Shao, M., Fu, L. L., Lu, S. H., Zeng, L. M., and Tang, D. G.: Source profiles of volatile organic compounds (VOCs) measured in China: Part I, Atmos. Environ., 42, 6247–6260, doi:10.1016/j.atmosenv.2008.01.070, 2008.

Lohmann, U. and Feichter, J.: Global indirect aerosol effects: a review, Atmos. Chem. Phys., 5, 715–737, doi:10.5194/acp-5-715-2005, 2005.

Makkonen, R., Asmi, A., Kerminen, V.-M., Boy, M., Arneth, A., Hari, P., and Kulmala, M.: Air pollution control and decreasing new particle formation lead to strong climate warming, Atmos. Chem. Phys., 12, 1515–1524, doi:10.5194/acp-12-1515-2012, 2012.

Merikanto, J., Spracklen, D. V., Mann, G. W., Pickering, S. J., and Carslaw, K. S.: Impact of nucleation on global CCN, Atmos. Chem. Phys., 9, 8601–8616, doi:10.5194/acp-9-8601-2009, 2009.

Metzger, A., Verheggen, B., Dommen, J., Duplissy, J., Prevot, A. S. H., Weingartner, E., Riipinen, I., Kulmala, M., Spracklen, D. V., Carslaw, K. S., and Baltensperger, U.: Evidence for the role of organics in aerosol particle formation under atmospheric conditions, P. Natl. Acad. Sci. USA, 107, 6646–6651, doi:10.1073/pnas.0911330107, 2010.

Mlawer, E. J., Taubman, S. J., Brown, P. D., Iacono, M. J., and Clough, S. A.: Radiative transfer for inhomogeneous atmospheres: RRTM, a validated correlated-*k* model for the longwave, J. Geophys. Res.-Atmos., 102, 16663–16682, doi:10.1029/97jd00237, 1997.

Myhre, G., Samset, B. H., Schulz, M., Balkanski, Y., Bauer, S., Berntsen, T. K., Bian, H., Bellouin, N., Chin, M., Diehl, T., Easter, R. C., Feichter, J., Ghan, S. J., Hauglustaine, D.,

ACPD
15, 27501–27538, 2015

Iversen, T., Kinne, S., Kirkevåg, A., Lamarque, J.-F., Lin, G., Liu, X., Lund, M. T., Luo, G., Ma, X., van Noije, T., Penner, J. E., Rasch, P. J., Ruiz, A., Seland, Ø., Skeie, R. B., Stier, P., Takemura, T., Tsigaridis, K., Wang, P., Wang, Z., Xu, L., Yu, H., Yu, F., Yoon, J.-H., Zhang, K., Zhang, H., and Zhou, C.: Radiative forcing of the direct aerosol effect from AeroCom Phase II simulations, Atmos. Chem. Phys., 13, 1853–1877, doi:10.5194/acp-13-1853-2013, 2013.

Nannoolal, Y., Rarey, J., and Ramjugernath, D.: Estimation of pure component properties – Part 3. Estimation of the vapor pressure of non-electrolyte organic compounds via group contributions and group interactions, Fluid Phase Equilibr., 269, 117–133, doi:10.1016/j.fluid.2008.04.020, 2008.

O'Dowd, C. D., Jimenez, J. L., Bahreini, R., Flagan, R. C., Seinfeld, J. H., Hameri, K., Pirjola, L., Kulmala, M., Jennings, S. G., and Hoffmann, T.: Marine aerosol formation from biogenic iodine emissions, Nature, 417, 632–636, doi:10.1038/Nature00775, 2002.

Paasonen, P., Sihto, S. L., Nieminen, T., Vuollekoski, H., Riipinen, I., Plass-Dulmer, C., Berresheim, H., Birmili, W., and Kulmala, M.: Connection between new particle formation and sulphuric acid at Hohenpeissenberg (Germany) including the influence of organic compounds, Boreal Environ. Res., 14, 616–629, 2009.

Qi, X. M., Ding, A. J., Nie, W., Petäjä, T., Kerminen, V.-M., Herrmann, E., Xie, Y. N., Zheng, L. F., Manninen, H., Aalto, P., Sun, J. N., Xu, Z. N., Chi, X. G., Huang, X., Boy, M., Virkkula, A., Yang, X.-Q., Fu, C. B., and Kulmala, M.: Aerosol size distribution and new particle formation in western Yangtze River Delta of China: two-year measurement at the SORPES station, Atmos. Chem. Phys. Discuss., 15, 12491–12537, doi:10.5194/acpd-15-12491-2015, 2015.

Schobesberger, S., Junninen, H., Bianchi, F., Lonn, G., Ehn, M., Lehtipalo, K., Dommen, J., Ehrhart, S., Ortega, I. K., Franchin, A., Nieminen, T., Riccobono, F., Hutterli, M., Duplissy, J., Almeida, J., Amorim, A., Breitenlechner, M., Downard, A. J., Dunne, E. M., Flagan, R. C., Kajos, M., Keskinen, H., Kirkby, J., Kupc, A., Kurten, A., Kurten, T., Laaksonen, A., Mathot, S., Onnela, A., Praplan, A. P., Rondo, L., Santos, F. D., Schallhart, S., Schnitzhofer, R., Sipila, M., Tome, A., Tsagkogeorgas, G., Vehkamaki, H., Wimmer, D., Baltensperger, U., Carslaw, K. S., Curtius, J., Hansel, A., Petaja, T., Kulmala, M., Donahue, N. M., and Worsnop, D. R.: Molecular understanding of atmospheric particle formation from sulfuric acid and large oxidized organic molecules, P. Natl. Acad. Sci. USA, 110, 17223–17228, doi:10.1073/pnas.1306973110, 2013.

Scott, C. E., Rap, A., Spracklen, D. V., Forster, P. M., Carslaw, K. S., Mann, G. W., Pringle, K. J., Kivekäs, N., Kulmala, M., Lihavainen, H., and Tunved, P.: The direct and indirect radia-

ACPD
15, 27501–27538, 2015

tive effects of biogenic secondary organic aerosol, Atmos. Chem. Phys., 14, 447–470, doi:10.5194/acp-14-447-2014, 2014.
Sihto, S.-L., Kulmala, M., Kerminen, V.-M., Dal Maso, M., Petäjä, T., Riipinen, I., Korhonen, H., Arnold, F., Janson, R., Boy, M., Laaksonen, A., and Lehtinen, K. E. J.: Atmospheric sulphuric acid and aerosol formation: implications from atmospheric measurements for nucleation and early growth mechanisms, Atmos. Chem. Phys., 6, 4079–4091, doi:10.5194/acp-6-4079-2006, 2006.
Sipila, M., Berndt, T., Petaja, T., Brus, D., Vanhanen, J., Stratmann, F., Patokoski, J., Mauldin, R. L., Hyvarinen, A. P., Lihavainen, H., and Kulmala, M.: The role of sulfuric acid in atmospheric nucleation, Science, 327, 1243–1246, doi:10.1126/science.1180315, 2010.
Volkamer, R., Jimenez, J. L., San Martini, F., Dzepina, K., Zhang, Q., Salcedo, D., Molina, L. T., Worsnop, D. R., and Molina, M. J.: Secondary organic aerosol formation from anthropogenic air pollution: rapid and higher than expected, Geophys. Res. Lett., 33, L17811, doi:10.1029/2006gl026899, 2006.
Wang, H. L., Zhu, B., Shen, L. J., An, J. L., Yin, Y., and Kang, H. Q.: Number size distribution of aerosols at Mt. Huang and Nanjing in the Yangtze River Delta, China: effects of air masses and characteristics of new particle formation, Atmos. Res., 150, 42–56, doi:10.1016/j.atmosres.2014.07.020, 2014.
Wang, M. and Penner, J. E.: Aerosol indirect forcing in a global model with particle nucleation, Atmos. Chem. Phys., 9, 239–260, doi:10.5194/acp-9-239-2009, 2009.
Wang, Z. B., Hu, M., Wu, Z. J., Yue, D. L., Zheng, J., Zhang, R. Y., Pei, X. Y., Paasonen, P., Dal Maso, M., Boy, M., and Wiedensohler, A.: Investigation of the connections between atmospheric new particle formation and organics at an urban site of Beijing, Atmos. Chem. Phys. Discuss., 13, 3419–3450, doi:10.5194/acpd-13-3419-2013, 2013a.
Wang, Z. B., Hu, M., Mogensen, D., Yue, D. L., Zheng, J., Zhang, R. Y., Liu, Y., Yuan, B., Li, X., Shao, M., Zhou, L., Wu, Z. J., Wiedensohler, A., and Boy, M.: The simulations of sulfuric acid concentration and new particle formation in an urban atmosphere in China, Atmos. Chem. Phys., 13, 11157–11167, doi:10.5194/acp-13-11157-2013, 2013b.
Weber, R. J., McMurry, P. H., Mauldin, R. L., Tanner, D. J., Eisele, F. L., Clarke, A. D., and Kapustin, V. N.: New particle formation in the remote troposphere: a comparison of observations at various sites, Geophys. Res. Lett., 26, 307–310, doi:10.1029/1998gl900308, 1999.

ACPD
15, 27501–27538, 2015

Wu, Z. J., Hu, M., Lin, P., Liu, S., Wehner, B., and Wiedensohler, A.: Particle number size distribution in the urban atmosphere of Beijing, China, Atmos. Environ., 42, 7967–7980, doi:10.1016/j.atmosenv.2008.06.022, 2008.

Xiao, S., Wang, M. Y., Yao, L., Kulmala, M., Zhou, B., Yang, X., Chen, J. M., Wang, D. F., Fu, Q. Y., Worsnop, D. R., and Wang, L.: Strong atmospheric new particle formation in winter in urban Shanghai, China, Atmos. Chem. Phys., 15, 1769–1781, doi:10.5194/acp-15-1769-2015, 2015.

Yli-Juuti, T., Nieminen, T., Hirsikko, A., Aalto, P. P., Asmi, E., Hõrrak, U., Manninen, H. E., Patokoski, J., Dal Maso, M., Petäjä, T., Rinne, J., Kulmala, M., and Riipinen, I.: Growth rates of nucleation mode particles in Hyytiälä during 2003–2009: variation with particle size, season, data analysis method and ambient conditions, Atmos. Chem. Phys., 11, 12865–12886, doi:10.5194/acp-11-12865-2011, 2011.

Yu, F. and Luo, G.: Simulation of particle size distribution with a global aerosol model: contribution of nucleation to aerosol and CCN number concentrations, Atmos. Chem. Phys., 9, 7691–7710, doi:10.5194/acp-9-7691-2009, 2009.

Yue, D. L., Hu, M., Zhang, R. Y., Wang, Z. B., Zheng, J., Wu, Z. J., Wiedensohler, A., He, L. Y., Huang, X. F., and Zhu, T.: The roles of sulfuric acid in new particle formation and growth in the mega-city of Beijing, Atmos. Chem. Phys., 10, 4953–4960, doi:10.5194/acp-10-4953-2010, 2010.

Zhang, Q., Stanier, C. O., Canagaratna, M. R., Jayne, J. T., Worsnop, D. R., Pandis, S. N., and Jimenez, J. L.: Insights into the chemistry of new particle formation and growth events in Pittsburgh based on aerosol mass spectrometry, Environ. Sci. Technol., 38, 4797–4809, doi:10.1021/Es035417u, 2004.

Zhang, R. Y., Suh, I., Zhao, J., Zhang, D., Fortner, E. C., Tie, X. X., Molina, L. T., and Molina, M. J.: Atmospheric new particle formation enhanced by organic acids, Science, 304, 1487–1490, doi:10.1126/science.1095139, 2004.

Zhou, L., Gierens, R., Sogachev, A., Mogensen, D., Ortega, J., Smith, J. N., Harley, P. C., Prenni, A. J., Levin, E. J. T., Turnipseed, A., Rusanen, A., Smolander, S., Guenther, A. B., Kulmala, M., Karl, T., and Boy, M.: Contribution from biogenic organic compounds to particle growth during the 2010 BEACHON-ROCS campaign in a Colorado temperate needleleaf forest, Atmos. Chem. Phys., 15, 8643–8656, doi:10.5194/acp-15-8643-2015, 2015.

Zhou, L. X., Nieminen, T., Mogensen, D., Smolander, S., Rusanen, A., Kulmala, M., and Boy, M.: SOSAA – a new model to simulate the concentrations of organic vapours, sulphuric acid and

ACPD
15, 27501–27538, 2015

aerosols inside the ABL – Part 2: Aerosol dynamics and one case study at a boreal forest site, Boreal Environ. Res., 19, 237–256, 2014.

ACPD
15, 27501–27538, 2015

Table 1. Chemical species from WRF-Chem inputted to MALTE-BOX.

WRF-Chem	MALTE-BOX
Acetaldehyde (CCHO)	CH3CHO
Acetone (ACET)	CH3COCH3
Methanol (MEOH)	CH3OH
Methyl Vinyl Ketone (MVK)	MVK
Isoprene (ISOPRENE)	C5H8
Terpenes (TERP)	alpha-pinene
	beta-pinene
	camphene
	myrcene
	carene
	limonene

ACPD
15, 27501–27538, 2015

Table 2. Formation rate of 6-nm particles (J_6), and particle growth rates from 6 to 30 nm (GR_{6-30}) of 3 NPF events based on DMPS measurements and numeric modelling*.

	Date	J_6 ($cm^{-3}\,s^{-1}$)	GR_{6-30} ($nm\,h^{-1}$)	CS ($10^{-2}\,s^{-1}$)
Case1	22 Jun 2013	7.6 (9.3)	12.6 (6.9)	4.2
Case2	10 Jul 2013	1.2 (1.6)	13.5 (10.7)	3.2
Case3	22 Aug 2013	3.4 (10.0)	15.7 (2.3)	0.1

* Values out of the parentheses are observations and those in the parentheses represent the corresponding model results.

ACPD
15, 27501–27538, 2015

Table 3. Statistical analyses of the simulated hourly 2 m temperature and 10 m wind speed vs. the ground observations at the SORPES station.

Date	Index*	2 m temperature (°C)	10 m wind speed ($m s^{-1}$)
22 Jun	MB	−0.33	0.80
	RMSE	1.29	1.63
10 Jul	MB	−1.07	−0.77
	RMSE	1.34	1.18
22 Aug	MB	0.19	0.17
	RMSE	1.38	1.27

* MB and RMSE refer to mean bias and root mean square error respectively.

ACPD
15, 27501–27538, 2015

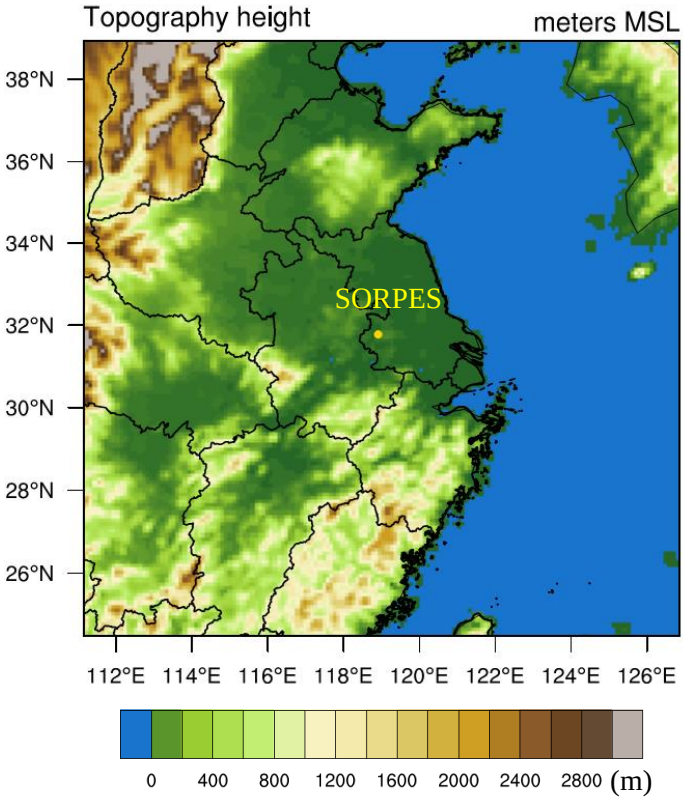

Figure 1. WRF-Chem model domain and topographic field (meter). The yellow dot marks the location of the SORPESstation.

ACPD
15, 27501–27538, 2015

First comprehensive modelling study on observed new particle formation

X. Huang et al.

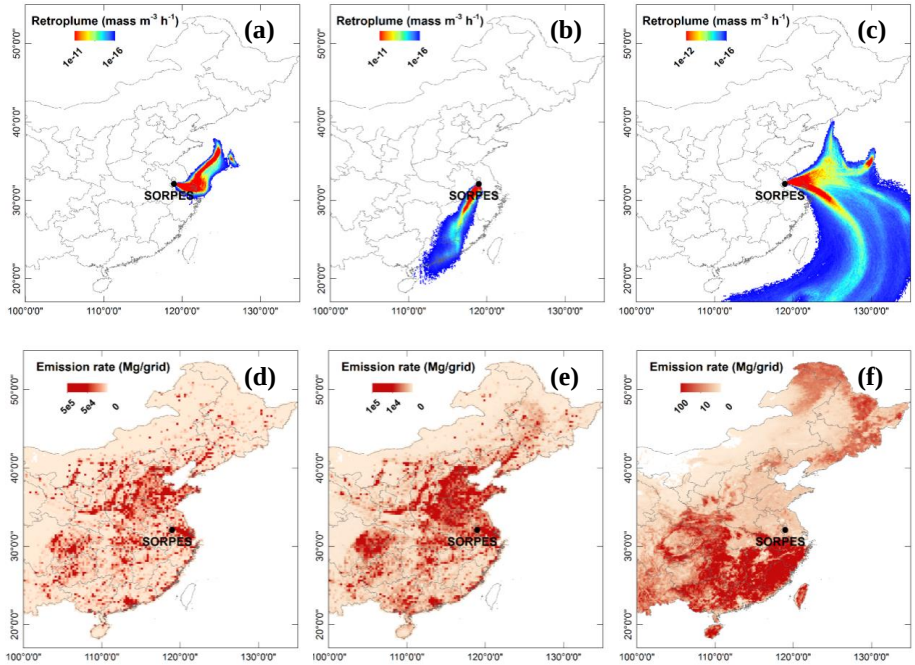

Figure 2. Retroplume (footprint residence time) showing transport pathways of air masses measured at the SORPES site for 22 June **(a)**, 10 July **(b)** and 22 August **(c)**. Spatial distributions of anthropogenic SO_2 **(d)**, primary $PM_{2.5}$ **(e)** and biogenic monoterpene **(f)** emission rates.

ACPD
15, 27501–27538, 2015

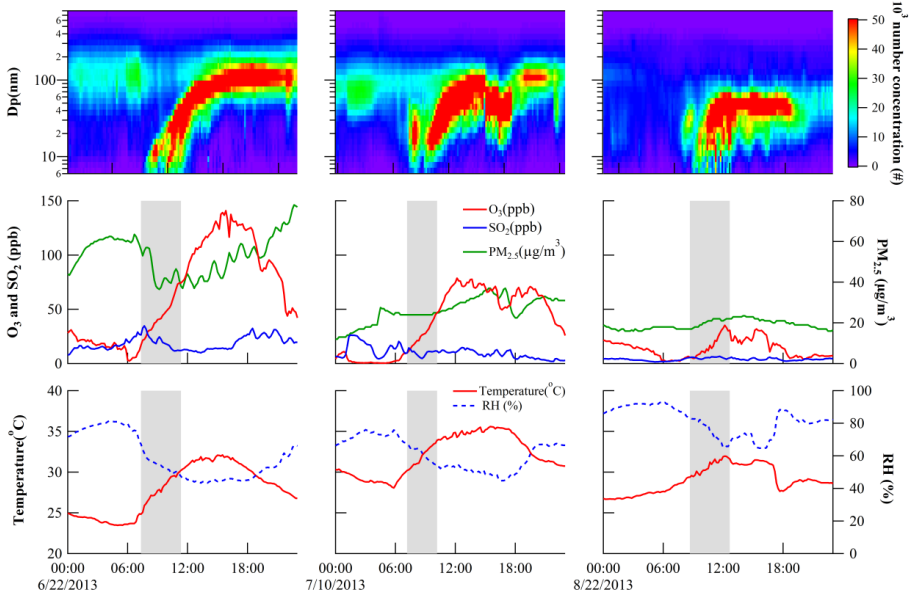

Figure 3. Measured diurnal variations of particle size distributions (upper panel), concentrations of SO_2, O_3 and $PM_{2.5}$ (middle panel), and meteorological conditions (bottom panel) during the three NPF days. Grey boxes show the time span of NPF events.

ACPD
15, 27501–27538, 2015

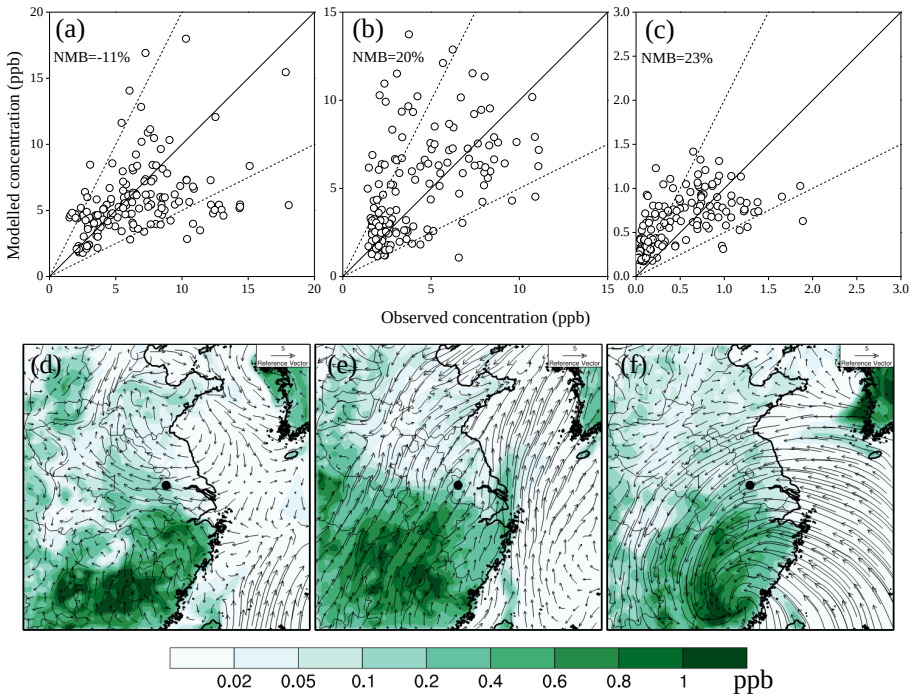

Figure 4. Scatter plots of observed and simulated alkene **(a)** aromatic **(b)** and isoprene **(c)** concentrations (NMB represents the normalized mean bias) in August 2014. Spatial distributions of terpene concentration at 09:00 LT on 22 June **(d)**, 10 July **(e)**, and 22 August **(f)**, 2013. The black dot marks the location of the SORPES station.

ACPD
15, 27501–27538, 2015

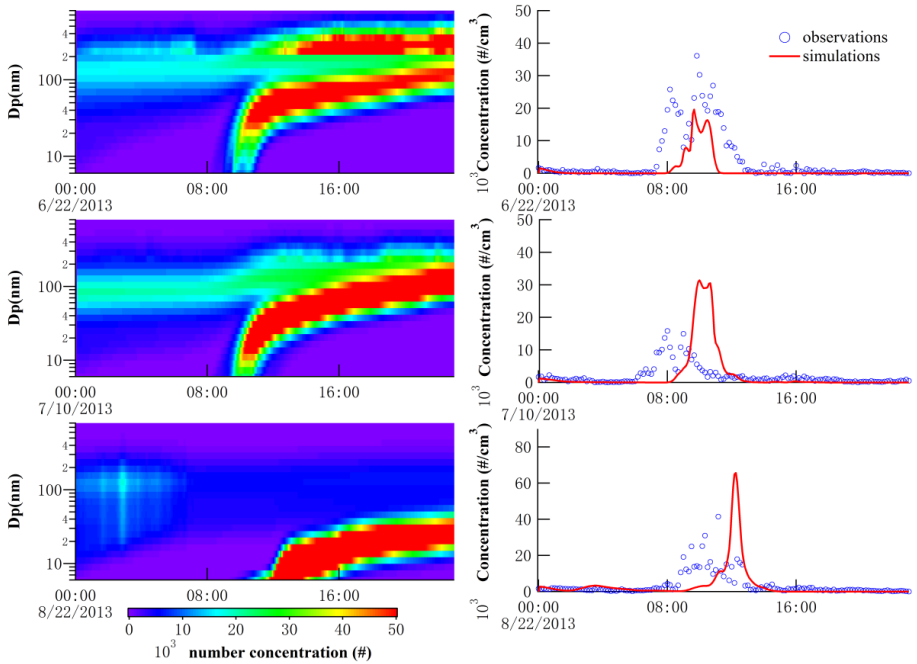

Figure 5. Modelled pattern of particle size distributions (left panel) and number concentrations of particles ranging from 6 to 10 nm during these 3 NPF days (right panel).

ACPD
15, 27501–27538, 2015

First comprehensive modelling study on observed new particle formation

X. Huang et al.

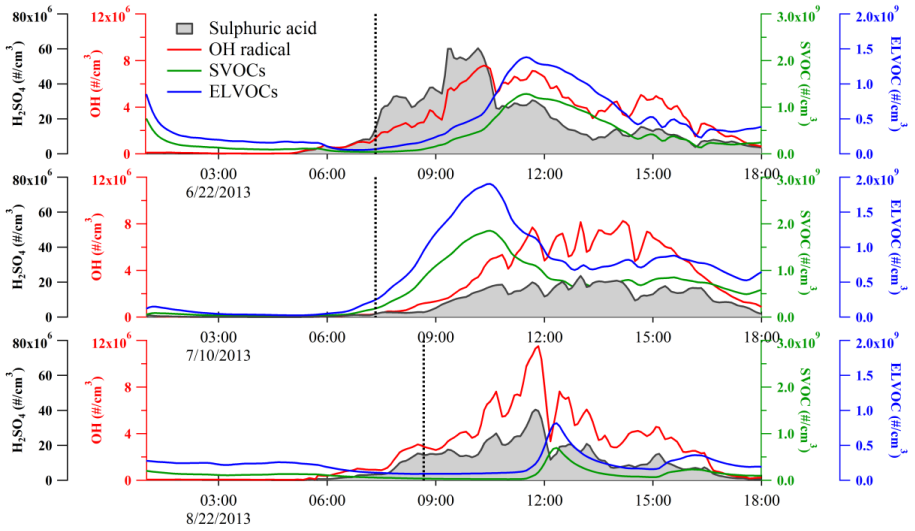

Figure 6. Time series of several gas concentrations (# cm^{-3}) during the three selected NPF days. Sulphuric acid, OH radical, SVOCs and ELVOCs are marked in grey area, red, green and blue lines, respectively. Dashed lines show the onset time of NPF according to DMPS measurements for reference.

ACPD
15, 27501–27538, 2015

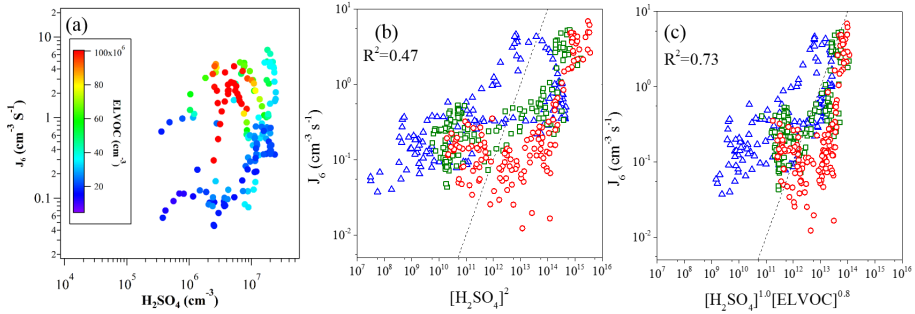

Figure 7. Correlations of estimated nucleation rates (J_6) from DMPS measurements with modelled gaseous sulphuric acid and ELVOC concentrations for event days between 06:00 and 16:00 **(a)**. Scatter plots of nucleation rate J_6 estimated from measurements with modelled sulphuric acid and ELVOC concentrations **(b–c)**, in which red, blue and green markers refer to 22 June, 10 July and 22 August, respectively. Black dash lines denote $y = 10^{-13}x$. The square of correlation coefficients (R^2) are labeled in panels **(b)** and **(c)**.

ACPD
15, 27501–27538, 2015